http://www.informaworld.com/smpp/260025382-92513912/content~db=all~content=a777900937

This article was downloaded by: *[INSTITUTO NACIONAL DE PESQUISAS ESPACIAIS]*
On: *23 April 2010*
Access details: *Access Details: [subscription number 915935802]*
Publisher *Taylor & Francis*
Informa Ltd Registered in England and Wales Registered Number: 1072954 Registered office: Mortimer House, 37-41 Mortimer Street, London W1T 3JH, UK

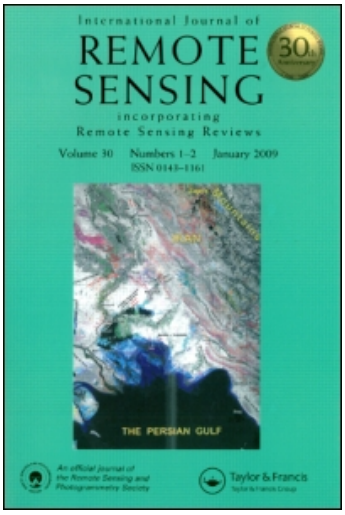

International Journal of Remote Sensing
Publication details, including instructions for authors and subscription information:
http://www.informaworld.com/smpp/title~content=t713722504

Comparison of fire detection in savannas using AVHRR's channel 3 and TM images

A. C. Pereira Jr [a];A. W. Setzer [a]
[a] INPE/DSR C, SP, Brazil

To cite this Article Pereira Jr, A. C. andSetzer, A. W.(1996) 'Comparison of fire detection in savannas using AVHRR's channel 3 and TM images', International Journal of Remote Sensing, 17: 10, 1925 — 1937
To link to this Article: DOI: 10.1080/01431169608948748
URL: http://dx.doi.org/10.1080/01431169608948748

PLEASE SCROLL DOWN FOR ARTICLE

Full terms and conditions of use: http://www.informaworld.com/terms-and-conditions-of-access.pdf

This article may be used for research, teaching and private study purposes. Any substantial or systematic reproduction, re-distribution, re-selling, loan or sub-licensing, systematic supply or distribution in any form to anyone is expressly forbidden.

The publisher does not give any warranty express or implied or make any representation that the contents will be complete or accurate or up to date. The accuracy of any instructions, formulae and drug doses should be independently verified with primary sources. The publisher shall not be liable for any loss, actions, claims, proceedings, demand or costs or damages whatsoever or howsoever caused arising directly or indirectly in connection with or arising out of the use of this material.

INT. J. REMOTE SENSING, 1996, VOL. 17, NO. 10, 1925–1937

Comparison of fire detection in savannas using AVHRR's channel 3 and TM images

A. C. PEREIRA JR and A. W. SETZER
INPE/DSR C. Postal 515, 12201-970, S.J. Campos, SP-Brazil

(*Received 11 July 1994, in final form 6 November 1995*)

Abstract. Detection of active fires in NOAA-11 AVHRR channel 3 (3·75 μm) afternoon images for an area of savannas in central Brazil was studied in relation to fire scars in Landsat TM images. Three consecutive TM images of the same area thus covering two periods of 16 days provided the 'ground truth' for the comparison of fire detection in AVHRR images of 15 and 14 days in each period. Using TM data as reference, 57 per cent of the new fire scars were associated with fires in channel 3 at the same places, in the first period. Seventy-four per cent of the active fires detected by AVHRR were verified in the TM imagery while the remainder was associated mainly with agricultural areas burned before the first period. For the second period, percentages were 53 per cent and 36 per cent respectively; the high percentage of unverified fires occurred mainly in grassland areas previously burned. Reasons for these results are discussed, namely, reflective soils in AVHRR's channel 3, fire scars not detected by TM because of precipitation, wind and fast changes in soil surfaces, and fires not active, or covered by clouds during AVHRR overpasses. A regression equation between the areas of the AVHRR fire pixels and of TM fire scars is also presented for the study area.

Downloaded By: [INSTITUTO NACIONAL DE PESQUISAS ESPACIAIS] At: 18:43 23 April 2010

1. Introduction

Biomass burning is normally associated with harmful local environmental consequences and introduces a significant amount of gases and aerosols in the troposphere. Current estimates suggest that on a global basis it could account for 1600–4100 $\times 10^{12}$ g of CO_2 per year and to 30–80 per cent of the total CO_2 emissions. Tropical savannas are known to burn with excessive recurrence caused by anthropogenic activity and the resulting tropospheric emissions contribute with a significant 29 per cent of total biomass burning emissions (Crutzen and Andreae 1990). Vegetation fires occur in most continental areas of the globe at rather unpredictable conditions and extent, which makes the use of remote sensing from space an attractive approach to their much needed detection and monitoring on a continuous and world-wide scale.

A real-time operational system to detect and fight fires using the 3·7 μm channel 3 of the Advanced Very High Resolution Radiometer (AVHRR) on-board National Oceanic and Atmospheric Administration (NOAA) series satellites was developed in Brazil and has been used since 1987 (Setzer and Pereira 1991, Setzer *et al.* 1992, Setzer 1993). A global fire product also based on AVHRR imagery is currently being considered (IGBP 1990). However, AVHRR was not designed for fire detection and its nominal saturation temperature of about 47° C in channel 3 is adequate mainly for ocean and cloud temperature monitoring. Its potential for fire detection, specifically that of channel 3 with its high sensitivity in the 400–700° C range, was pointed already in Dozier (1981) but little AVHRR fire validation work is found in the

0143–1161/96 $12.00 © 1996 Taylor & Francis Ltd

literature. Setzer and Pereira (1991) and Setzer *et al.* (1992) refer to 98 per cent of verification hits by fire brigades in operational activities, but with no reference to area estimates. Setzer *et al.* (1994) describe the AVHRR response for two prescribed fires in a tropical forest environment, and Belward *et al.* (1993) for five fires in west Africa savannas. Pereira Jr *et al.* (1991) worked with a savanna test area of about 17 000 km^2 in central Brazil and verified AVHRR channel 3 detection of fires during a period between two consecutive Landsat TM overpasses in the same area; all AVHRR fires detected were verified in the TM imagery, and 35 per cent of all fire scars in the TM imagery did not have a corresponding fire pixel in the AVHRR data.

High resolution data like Thematic Mapper (TM) images from the Landsat satellites are one of the potential possibilities to analyse AVHRR detection of fires. Fire detection with AVHRR channel 3 data at night-time is a straight-forward procedure because the ground reflected signal in the band does not exist. However, most vegetation fires, particularly in savannas (e.g., Coutinho 1990 and Langaas 1992), are caused by humans mainly during daytime.

This paper presents an effort to understand and validate AVHRR fire detection through the comparison of AVHRR and TM results in the type of vegetation environment which presents the most extreme difficulties for AVHRR fire detection at daytime. AVHRR is still the only satellite tool used to detect fires on regular daily programmes, and it has proved to be extremely useful for forest and dense vegetation environments. In order to extend its use also to the savannas of the world in a reliable way, validation work is needed specifically for this ecosystem. Because no such validation can be found in the literature the results below present novel information.

2. Area of study and satellite data

A study area having the following requirements was selected:

1. To include the main vegetation patterns that occur in the central Brazilian savannas, generically known as *cerrados*, ranging from savanna grassland (*campo sujo*) to sclerophyllous woodland (*cerradão*), either in their natural conditions or modified by anthropic actions.
2. To be located in a single Landsat TM image frame (185 km by 185 km).
3. To be imaged in three consecutive Landsat TM passes with very little cloud cover, therefore covering two periods of 16 days in the dry/fire season.

The IBGE/IBDF (1988) vegetation map and the Brazilian National Space Research Institute—INPE archive of TM images were examined, and the TM images selected were those of 26 August, 11 September and 27 September 1989, path 223, row 69, with cloud cover of 20, 10, and 10 per cent, respectively. This scene corresponds to the area between the latitudes of 12° 05′ S to 14° 00′ S and the longitudes of 49° 20′ W and 51° 30′ W. Its size, of about 34 225 km^2, corresponds to 1·6 per cent of the estimated 2·2 million km^2 of cerrados in Brazil. This area, shown in figure 1, has flat or gently rolling tablelands with elevation between 200 and 600 m, and includes most of the cerrado vegetation types, being subject to the cerrado anthropogenic fire regime (Azevedo e Adámoli 1988, Coutinho 1990). Average annual precipitation in the region is about 1800 mm of which 10 per cent in the dry months of July–September (Espinoza *et al.* 1982). No meteorological data for the region could be located relative to the two study periods, and the three closest weather stations

Downloaded By: [INSTITUTO NACIONAL DE PESQUISAS ESPACIAIS] At: 18:43 23 April 2010

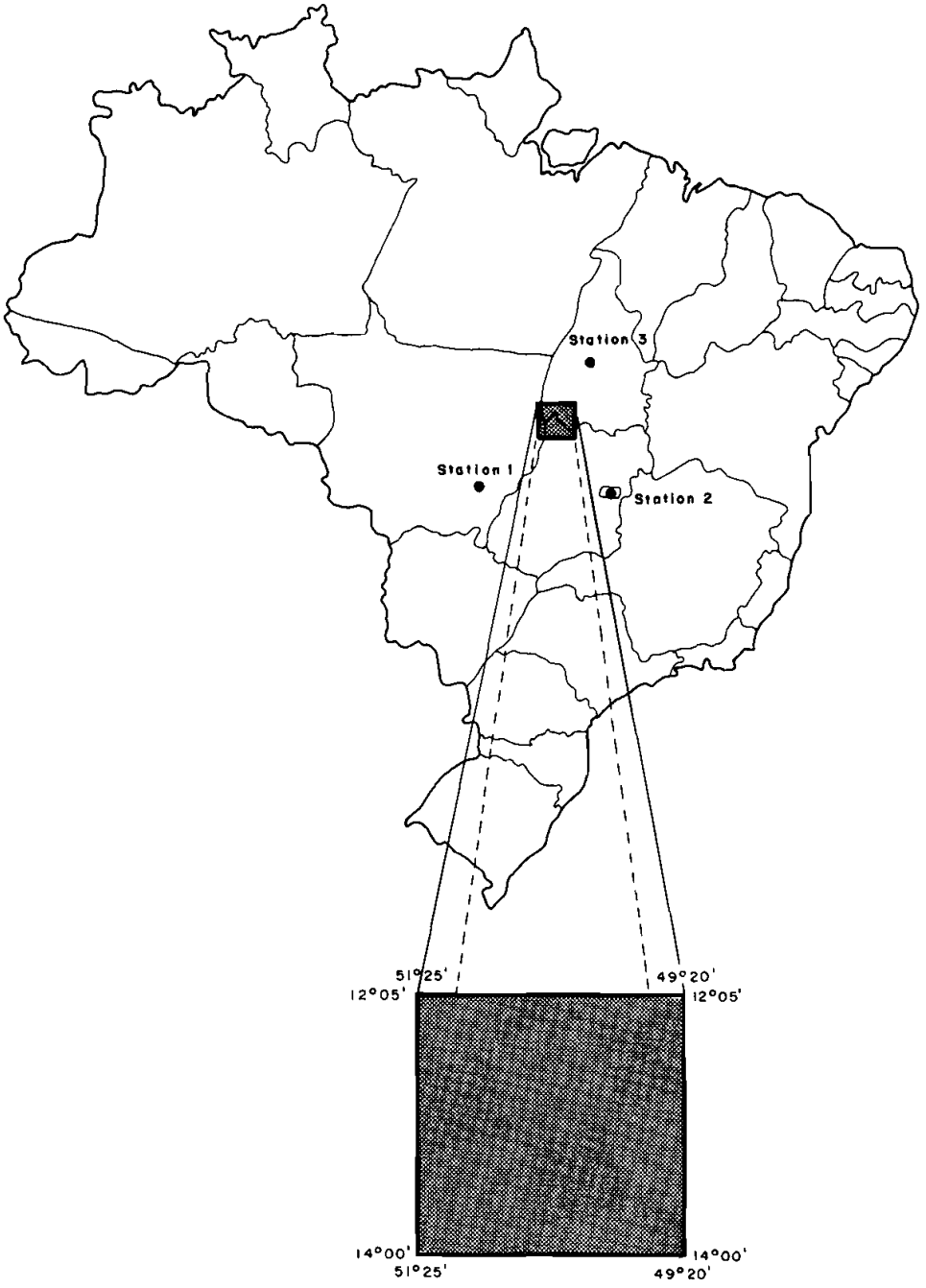

Figure 1. Study area with closest weather stations.

found are shown in figure 1. Precipitation registered at these stations is given in table 1, indicating that the study periods were subject to a mild dry season.

The AVHRR afternoon images (figure 2(*a*)) used were those of the NOAA-11 satellite (Kidwell 1991), normally recorded by INPE for the operational near-real-

Downloaded By: [INSTITUTO NACIONAL DE PESQUISAS ESPACIAIS] At: 18:43 23 April 2010

Table 1. Precipitation (mm) and cloud cover (%) data for three weather stations close to the study area.

Days	Station 1 15°38'S 53°54'W	Station 2 15°47'S 47°56'W	Station 3 10°31'S 48°43'W	Cloud cover
First period				
25 August	0	0	0	—
26 August	25	1	0	75
27 August	0	3	1	100
28 August	4	10	0	100
29 August	0	6	0	100
30 August	0	0	0	0
31 August	36	0	0	0
1 September	1	0	0	0
2 September	2	0	0	50
3 September	1	0	0	100
4 September	0	0	0	75
5 September	16	24	12	100
6 September	2	11	0	100
7 September	2	11	0	50
8 September	2	6	3	25
9 September	2	5	3	—
10 September	2	0	6	75
Second period				
11 September	2	0	6	75
12 September	2	0	6	75
13 September	3	0	1	100
14 September	3	0	1	75
15 September	3	0	1	75
16 September	0	0	0	25
17 September	0	0	0	0
18 September	0	0	0	50
19 September	0	18	0	100
20 September	0	11	2	100
21 September	0	4	4	100
22 September	0	0	3	—
23 September	0	0	0	—
24 September	0	0	0	75
25 September	1	0	4	75
26 September	0	0	0	75

See figure 1 for the location of the three meteorological station. Cloud cover was obtained from the AVHRR images.

time detection of fires in Brazil. Channels recorded in the High Resolution Picture Transmission—HRPT mode at full resolution by INPE at the time were 1 (0·58–0·68 μm), 2 (0·73–1·1 μm), and 3 (3·55–3·93 μm). The 15 images used in the first period were from 26 August through 10 September 1989, with the exception of 9 September due to problems in the receiving station. The AVHRR image of 11 September was not used in this period because the TM overpass is in the morning (09:45 local time), before the AVHRR afternoon overpass. For the second period 14 AVHRR images were used, covering 11 September through 26 September 1989, except for 22 and 23 September also because of hardware problems. Table 2 shows the equatorial crossing longitude and time for the NOAA-11 overpasses used, and

Downloaded By: [INSTITUTO NACIONAL DE PESQUISAS ESPACIAIS] At: 18:43 23 April 2010

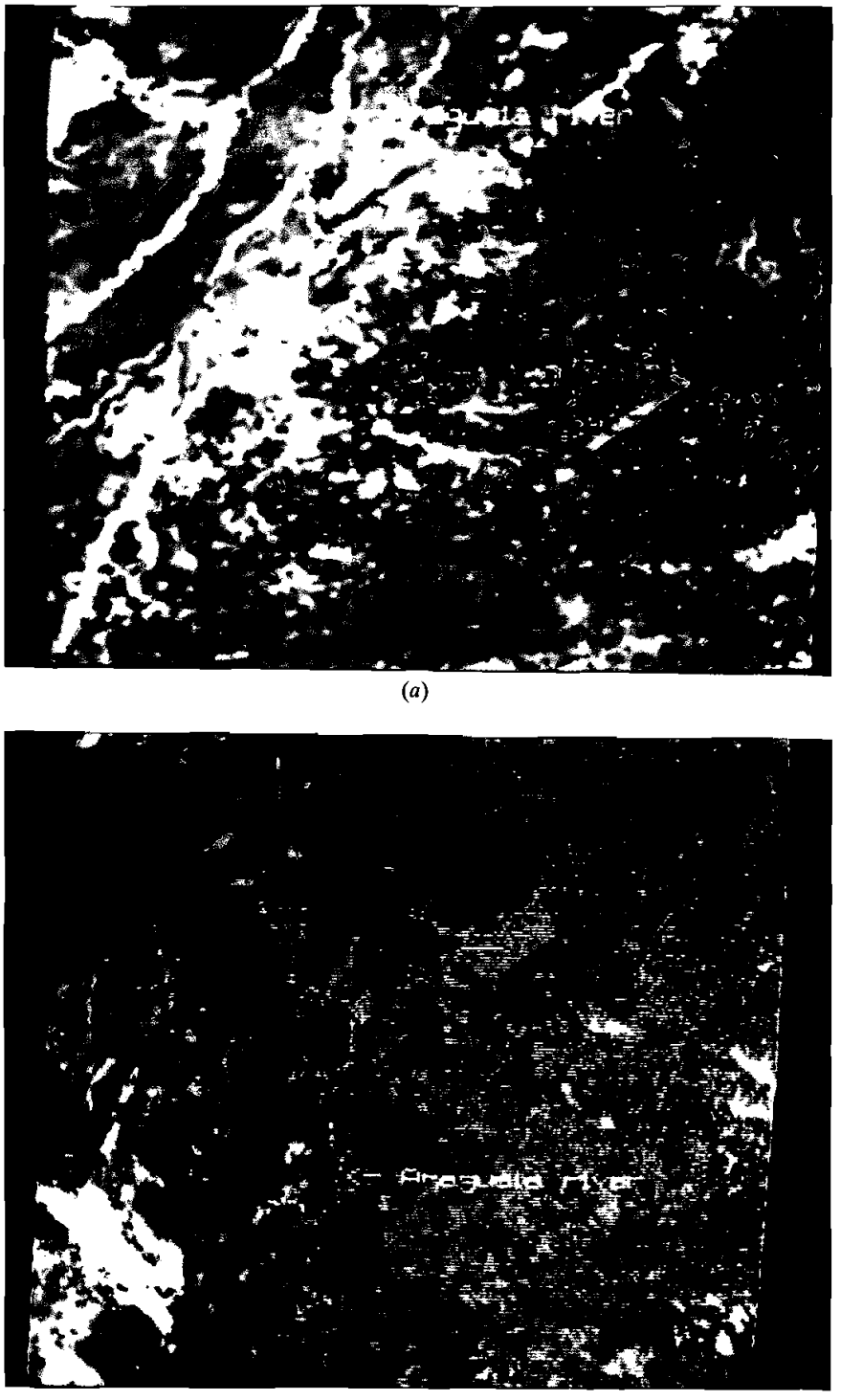

(*a*)

(*b*)

Figure 2. (*a*) Channel 3 of AVHRR afternoon image of 31 September 1989 showing fire pixels in yellow. (*b*) Colour composition of channels 3, 4 and 5 of Landsat TM image of 11 September 1989, for orbit 223/69, showing fire scars in yellow.

Downloaded By: [INSTITUTO NACIONAL DE PESQUISAS ESPACIAIS] At: 18:43 23 April 2010

Table 2. AVHRR/NOAA-11 images used in the study.

Dates	Equatorial crossing		Distance from nadir		Pixel area (km^2)
	Long.	Hour	Columns	km	
First period					
26 August	295·6	18:08:03	944	1247	6·02
27 August	298·2	17:57:31	874	957	4·11
28 August	300·9	17:46:58	696	657	2·11
29 August	303·5	17:36:26	396	367	1·13
30 August	306·2	17:25:53	76	67	0·88
31 August	308·8	17:15:20	250	223	0·97
1 September	311·5	17:04:47	484	523	1·30
2 September	314·1	16:54:14	715	813	2·23
3 September	316·8	16:43:41	884	1113	4·32
4 September	293·9	18:15:14	964	1436	6·84
5 September	296·6	18:04:41	911	1136	4·97
6 September	299·2	17:54:08	829	846	3·36
7 September	301·9	17:43:35	596	545	1·62
8 September	304·5	17:33:01	318	256	1·03
9 September	—	—	—	—	—
10 September	309·8	17:11:54	351	334	1·07
Second period					
11 September	312·5	17:01:21	590	635	1·60
12 September	315·1	16:50:47	799	924	2·98
13 September	317·8	16:40:13	944	1224	5·87
14 September	294·9	18:11:46	959	1325	6·62
15 September	297·6	18:01:12	904	1024	4·78
16 September	300·2	17:50:38	754	735	2·53
17 September	302·9	17:40:04	484	434	1·30
18 September	305·5	17:29:30	136	145	0·90
19 September	308·2	17:18:56	205	156	0·94
20 September	310·9	17:08:21	445	456	1·22
21 September	313·6	16:57:44	645	757	1·83
22 September	—	—	—	—	—
23 September	—	—	—	—	—
24 September	295·9	18:07:26	914	1213	5·05
25 September	298·6	17:56:51	864	913	3·92
26 September	301·3	17:46:15	654	612	1·87

the distance between the centre of the study area and the image nadir in kilometres and pixel columns.

Digital processing was done using only the eight most significant bits (256 grey levels) of the original 10-bit (1024 levels) HRPT image. Fire pixels in the AVHRR images were considered to be all channel 3 pixels with digital count (DN) between 0 and 10 in the 256-level scale used, corresponding to DNs 0–43 in the 10-bit scale. This histogram thresholding procedure follows the findings of Pereira and Setzer (1993 a) which have been field verified (Setzer and Pereira 1991). The threshold limit actually changes with time and the value used is in agreement with results reported for fires in other parts of the world at that time (Setzer and Malingreau 1993). Areas of individual fire events in channel 3 were obtained by adding the area of all fire pixels in each event and accounting for the geometrical distortion of pixels caused

Downloaded By: [INSTITUTO NACIONAL DE PESQUISAS ESPACIAIS] At: 18:43 23 April 2010

by off-nadir viewing effects. The area of the AVHRR pixel at nadir used was 0·876 km^2, corresponding to a pixel with 803 m by 1091 m, and not the value of 1·21 km^2 commonly found in the literature for a nominal square pixel with a side of 1·1 km. The latter results when the pixel size is calculated based only on the AVHRR instantaneous field-of-view (IFOV), while the former deducts the overlap of adjacent pixels.

Channels TM3 (0·63–0·69 μm), TM4 (0·76–0·90 μm) and TM5 (1·55–1·75 μm) of the three TM images (figure 2(*b*)) were used in this work to estimate the extent of burned areas after the results of Ponzoni *et al.* (1986), Pereira (1992) and Pereira and Setzer (1993 b). A Vegetation Index (VI) was obtained from channels 3 and 4, using the relation (TM4 − TM3)/(TM4 + TM3) and was also used in the analysis. The identification of fire scars was made by digital classification with the so-called parallelepiped algorithm, using channels VI, 4 and 5. The VI channel was used in order to reduce the confusion of ground covers with exposed soils or with soils where the vegetation was burned before the date of the first TM image (Chuvieco and Congalton 1988). The area of individual fire scars was automatically obtained from the image processing system used (Engespaço 1988), multiplying the number of TM pixels in this class by their unit area of 0·009 km^2.

The fire scars detected in the TM images were plotted in standard maps in the 1 : 100 000 scale to find their approximate geographical location. The plotting was based on the identification of significant landmarks close to the fire scars, such as rivers, lakes, roads and hills noticeable in the maps and in the TM images. The accretion of the numbers of new fire scars in each of the two periods was determined from the visual comparison of the consecutive and classified TM digital images for each of the two periods of study. The geographical location of the fire pixels in the AVHRR images was also found based on the position of close and significant land marks; the TM images were also used to help the identification of the land marks in the AVHRR images. This method resulted in a more precise location than the use of navigation algorithms in the image processing system.

3. Results and discussion

Table 3 shows the correspondence between fire scars which occurred during the two 16-day interval periods of the three TM images used and active fires detected in the AVHRR channel 3 images of 15 and 14 days during the same intervals and for the same region of cerrado vegetation. Data are listed for each period in numerical order of the sizes of the fire scar area in the TM column. Zero values in the table indicate that the fire event was not detected by the satellite relative to the respective column. The two AVHRR columns of data for each period present the number of AVHRR pixels associated with each fire event and the area covered by these pixels. The last column contains the number of images (days) in which the same fire was detected. In the case of small fires, with less than 3 km^2 in the TM images, which last only a few hours at the most, their indication in more than one image (day) is a clear result of solar reflection from soils that became exposed after the fire removed their short vegetation cover. It must be stressed that direct comparison of TM and AVHRR areas in this context is not possible. In addition to the solar reflection problem in channel 3 just exemplified, areas of fire scars in the TM images basically show the total extent of fire events after their end. AVHRR data, on the other hand, represent only an instantaneous view of fires at the satellite overpass time, and in principle should only be associated with fire fronts. Furthermore, AVHRR pixel

Downloaded By: [INSTITUTO NACIONAL DE PESQUISAS ESPACIAIS] At: 18:43 23 April 2010

Table 3. Comparison of fire events in Landsat TM and AVHRR/NOAA images.

Case no.	TM area (km^2)	AVHRR No. of pixel	AVHRR area (km^2)	No. of images	Case no.	TM area (km^2)	AVHRR No. of pixel	AVHRR area (km^2)	No. of images
First period									
1	0·000	1	0·9	1	53	1·045	0	0·0	—
2	0·000	1	1·2	1	54	1·077	0	0·0	—
3	0·000	1	1·2	1	55	1·077	2	1·8	1
4	0·000	1	1·2	1	56	1·697	1	2·0	1
5	0·000	2	1·8	1	57	1·743	2	2·0	1
6	0·000	2	2·5	2	58	1·755	0	0·0	—
7	0·000	2	2·5	1	59	1·873	0	0·0	—
8	0·000	4	2·6	3	60	1·903	6	5·1	1
9	0·000	2	2·8	2	61	2·101	0	0·0	—
10	0·000	2	3·1	1	62	2·277	0	0·0	—
11	0·000	2	3·1	1	63	2·378	3	5·3	2
12	0·000	2	3·1	1	64	2·452	4	3·8	3
13	0·000	3	3·7	1	65	2·764	6	23·0	3
14	0·000	2	9·4	1	66	2·889	0	0·0	—
15	0·000	11	13·3	3	67	3·131	0	0·0	—
16	0·028	0	0·0	—	68	3·235	0	0·0	—
17	0·034	0	0·0	—	69	3·434	0	0·0	—
18	0·052	0	0·0	—	70	3·908	1	1·6	1
19	0·062	0	0·0	—	71	4·200	1	1·6	1
20	0·088	0	0·9	1	72	4·256	3	9·6	2
21	0·089	0	0·0	—	73	4·829	3	4·3	2
22	0·096	0	0·0	—	74	5·762	7	7·0	2
23	0·099	2	2·0	2	75	6·087	0	0·0	—
24	0·134	3	4·1	2	76	6·541	3	3·1	1
25	0·144	1	1·2	1	77	7·892	4	4·1	2
26	0·162	2	4·3	1	78	8·267	18	21·4	4
27	0·166	0	0·0	—	79	9·204	0	0·0	—
28	0·168	1	1·6	1	80	9·458	28	26·1	4
29	0·203	0	0·0	—	81	10·143	11	15·0	2
30	0·205	2	1·7	1	82	11·012	3	4·7	1
31	0·216	3	3·7	1	83	14·511	27	28·0	4
32	0·219	7	16·2	3	84	14·716	35	37·2	4
33	0·262	0	0·0	—	85	15·573	12	21·9	3
34	0·302	0	0·0	—	86	16·164	7	25·0	3
35	0·336	0	0·0	—	87	16·402	16	15·8	1
36	0·382	2	6·4	1	88	24·484	51	66·8	5
37	0·383	0	0·0	1	89	25·520	61	80·5	5
38	0·396	5	10·0	3	90	44·120	65	72·8	3
39	0·452	0	0·0	—					
40	0·490	0	0·0	—	*Second period*				
41	0·508	4	7·2	2	1	0·000	1	1·2	1
42	0·519		2·0	1	2	0·000	1	1·2	1
43	0·520	0	0·0	—	3	0·000	1	1·2	1
44	0·571	0	0·0	—	4	0·000	1	1·2	1
45	0·599	2	2·5	2	5	0·000	2	2·5	1
46	0·610	0	0·0	—	6	0·000	3	2·9	2
47	0·696	0	0·0	—	7	0·000	3	3·0	2
48	0·703	2	2·0	1	8	0·000	2	3·0	1
49	0·879	9	10·4	4	9	0·000	3	3·7	1
50	0·940	6	5·6	2	10	0·000	3	3·7	1
51	0·965	0	0·0	—	11	0·000	3	3·7	1
52	0·992	0	0·0	—	12	0·000	4	4·2	2

Downloaded By: [INSTITUTO NACIONAL DE PESQUISAS ESPACIAIS] At: 18:43 23 April 2010

Table 3. (*continued*).

Case no.	TM area (km^2)	AVHRR No. of pixel	AVHRR area (km^2)	No. of images	Case no.	TM area (km^2)	AVHRR No. of pixel	AVHRR area (km^2)	No. of images
Second period									
13	0·000	4	4·3	2	36	0·279	0	0·0	—
14	0·000	4	5·0	1	37	0·285	0	0·0	—
15	0·000	5	5·8	2	38	0·297	3	5·6	2
16	0·000	3	6·2	2	39	0·323	0	0·0	—
17	0·000	8	7·2	2	40	0·384	4	4·9	2
18	0·000	2	7·4	1	41	0·397	0	0·0	—
19	0·000	4	7·4	2	42	0·424	0	0·0	—
20	0·000	7	11·4	5	43	0·491	0	0·0	—
21	0·000	8	13·2	3	44	0·494	43	75·1	6
22	0·000	22	24·3	5	45	0·883	2	3·6	1
23	0·000	26	29·9	5	46	1·211	0	0·0	
24	0·000	40	40·1	4	47	1·995	1	0·9	1
25	0·000	51	69·5	4	48	3·115	0	0·0	—
26	0·000	43	81·0	6	49	3·673	21	25·2	4
27	0·000	56	89·8	5	50	4·772	8	9·7	4
28	0·000	137	142·2	4	51	6·830	18	26·1	6
29	0·029	0	0·0	—	52	7·507	29	38·7	5
30	0·056	0	0·0	—	53	8·130	53	73·4	5
31	0·059	5	5·0	3	54	8·702	9	19·3	4
32	0·104	0	0·0	—	55	10·891	8	27·9	2
33	0·112	0	0·0	—	56	24·671	69	159·2	5
34	0·119	0	0·0	—	57	177·866	172	308·7	9
35	0·121	0	0·0	—					

radiometry and geometry bring additional restrictions: a fire pixel in channel 3 refers to any fire front larger than ~50 m (Setzer and Pereira 1991) up to the area covered by an IFOV (1·26 km^2 at nadir to 15·14 km^2 at the image edges), and neighbouring pixels have large overlaps, of at least of ~63 per cent. These facts pose insurmountable limitation to estimates of the size of individual fire events in AVHRR imagery.

The data in table 3 show that for the first period, 43 of the 58 active fires detected by AVHRR were verified in the TM images, or 74 per cent of the cases. 11 out of the 15 fires not verified occurred in areas of agricultural use, and the remaining 4 fires not verified were in *campo sujo* (grasslands). In addition, 11 fires that could not be verified in the TM image occurred in areas that were burned before 26 August. In the second period, 16 of the 45 active fires detected by AVHRR were verified, or 36 per cent of the cases. 27 out of 29 fires not verified occurred in *campo sujo* and 2 in agricultural areas; 19 of these cases occurred in areas burned in the first period and 2 occurred in areas burned by 26 August.

Explanations for these differences in the AVHRR and TM images are found mainly in four possibilities. First, AVHRR channel 3 is sensitive to reflected solar radiation from some exposed soils at specific reflection angles, which cause the same signal as active fires (Setzer and Verstraete 1994). Since no technique has been currently devised to differentiate fires from soil reflection, confusion of these two targets does take place to some extent. This can explain the increment in the number of fires in the second period located in areas previously burned.

Second, agricultural areas are usually ploughed or tilled after fires occur to take

Downloaded By: [INSTITUTO NACIONAL DE PESQUISAS ESPACIAIS] At: 18:43 23 April 2010

advantage of ashes rich in nutrients, and by the time the TM image is acquired the scar may not be identifiable any more. Third, winds and rains can disperse the thin layer of ashes making TM identification of fire scars difficult. Fourth, if some rain occurs in the cerrados, as was probably the case in this study (see table 1), vegetation in the areas that burned before the rains will sprout in a matter of one week, much faster than in areas not burned thus preventing the identification of fires scars in the TM images.

Even using digital classification processing and visual enhancement of the TM images the authors believe that misidentification of some fire scars in these types of vegetation, either affected or not by rains, could have occurred. The consequences of this limitation are of two types: (a) AVHRR classification indicates a false scar of a fire that never occurred, or (b) AVHRR detects a real fire that cannot be verified by TM. Such doubts could only be eliminated if both TM and AVHRR images were processed in real-time and ground crews could verify all fires in the field on a daily basis. Considering that the acquisition of three (or even two) consecutive TM images for a given area is a very rare case because of cloud cover, that it is impossible to know in advance when and where this sequence will be available and that the scene of a TM image has 34 225 km^2 where fires occur randomly, the possibilities of having fieldwork validation are minimal. Therefore, some margin of doubt will always exist in AVHRR fire validation with TM.

Also important in table 3 is the fact that a positive correlation can be found between the sizes of active fires in AVHRR channel 3 and those of corresponding fire scars in the TM images—see § 4 below for the statistical regression. For instance, in the first period the largest fire scars, with 25·5 km^2 and 44·1 km^2, were associated to the largest active fires in channel 3, which overestimated them with 61 and 65 fire pixels, or 80·5 km^2 and 72·5 km^2, respectively. This fact also occurred in the second period in which the largest fire scars with 24·7 km^2 and 177·9 km^2 were associated to the largest active fires, which overestimated them with 69 and 172 fire pixels, or 159·2 km^2 and 308·7 km^2, respectively. This area overestimate effect in channel 3 is also seen for smaller areas, as in the cases during the first period where the TM fire scar areas were 0·219 km^2 and 0·879 km^2 and AVHRR had 7 and 9 fire pixels associated, with corresponding areas of 16·2 km^2 and 10·4 km^2, respectively. In the second period for example, the TM fire scars with 0·059 km^2 and 0·384 km^2 were detected with 5 and 4 fire pixels by the AVHRR, with 5·0 km^2 and 4·9 km^2 respectively. These AVHRR overestimates are a combined result of factors already mentioned: soil reflection in days after the fire, overlap of neighbouring fire pixels which actually depict the same area, high sensitivity of channel 3 which registers small and large fires alike, and increased pixel sizes at off-nadir angles.

From table 3 we also conclude that in the first 16 days interval of the first two TM images a total of 75 fire events were detected through TM in the study area. Their size was 4·18 km^2 on the average, ranging from 0·028 to 44·12 km^2 and 75 per cent of the fires had less than 4·26 km^2. In the second 16 days interval a total of 30 fire scars were detected, with an average size of 9·11 km^2 ranging from 0·029 to 177·87 km^2, in which 75 per cent of the fires had less than 4·77 km^2. Considering the TM data as ground truth, in the first period 43 TM fire scars had corresponding AVHRR fire pixels, e.g., 57 per cent of the cases. For the second period of 16 days, 16 TM fire scars had corresponding AVHRR fire pixels, e.g., 53 per cent of the cases.

The relatively low percentages of fires detected by AVHRR are believed to result from two main reasons. First, fires not active during the satellite pass. Fires in the

Downloaded By: [INSTITUTO NACIONAL DE PESQUISAS ESPACIAIS] At: 18:43 23 April 2010

cerrados spread at high speeds with cooling of the burned areas in a matter of seconds (Ward *et al.* 1992), having strong chances of not being detected by a satellite instantaneous view. In a case of fire spreading in cerrados, during the Emas National Park great fire of 1988, when 776 km^2 burned as fire fronts progressed uncontrolled for 7 days, AVHRR fire pixels in the afternoon overpasses accounted only for 13 per cent of the area actually burned (Pereira *et al.* 1990). Therefore, for small areas burned as is the case of this study, chances that AVHRR does not detect them prevail, with the maximum area not detected of 9·20 km^2.

The second reason is the common presence of weather clouds during acquisition of the AVHRR images thus precluding detection of some active fires. Although fires are usually not lit in cloudy days to avoid poor combustion efficiency, isolated clouds in sunny days pose no such restriction and reduce fire detection by the satellite. As seen in table 1, of the 15 images of different days in the first period of 16 days, for 5 images (27, 28 and 29 August, 5 and 6 September) the cloud cover was 100 per cent in the study area; for 3 images (26 August, 4 and 10 September) the cloud cover was 75 per cent; and for 2 images (2 and 7 September) was 50 per cent. During the second period, of the 14 images of September, 4 images (days 13, 19, 20 and 21) had cloud cover of 100 per cent; in 7 images (days 11, 12, 14, 15, 24, 25 and 26), had 75 per cent; 1 image (day 18) had 50 per cent; and in 1 image (day 16) the cloud cover was 25 per cent.

4. AVHRR × TM statistical regression

Vegetation fires around the globe must be understood in terms of their excessive frequency and extent, and not as isolated cases. It is estimated that a third of the world savannas burn every year, and this figure may even increase depending on regional dryness conditions. Hundreds of thousands of independent fires take place every year in each of the major savannas ecosystems of the globe, in Africa, South America, Asia and Australia. In this context, considering such large numbers of fires, the lack of any source of information on the subject, and despite all limitations in fire comparison of AVHRR and TM data pointed above, the knowledge of relations between the area of fire scars in TM images and AVHRR fire pixels for specific region is a valid exercise.

Using the data from table 3 the following linear regression equations were found between the area in km^2 covered by fire pixels in AVHRR's channel 3 (AA3) and the area of fire scars measured in the TM images (ATM) for the same study area in the two periods analysed. In the first equation F-ratio is 193·8, highly significant and R^2, the correlation coefficient, 0·78. For the second equation, these values were 75·6 and 0·65, respectively.

$$1.\ AA3 = 1{\cdot}8 \times ATM + 2{\cdot}3, \quad \text{for the first period;}$$

$$2.\ AA3 = 1{\cdot}7 \times ATM + 21{\cdot}5 \quad \text{for the second period.}$$

The variation among the equations for the two periods show that large deviations exist even for the same region and that the use of such equations possibly provide nothing more than the order of magnitude of the area burned. Even so, AVHRR is the only existing approach to monitor vegetation fires on continental or global scales and such equations may after all provide useful insights to quantify biomass burning in remote regions.

Downloaded By: [INSTITUTO NACIONAL DE PESQUISAS ESPACIAIS] At: 18:43 23 April 2010

5. Conclusions

Inter-comparison of active fires in NOAA-AVHRR channel 3 low resolution images with fire scars in high resolution Landsat TM images presents insurmountable limitations for areas of savannas/cerrado vegetation. Small and quick fires, cloud cover, reflective soils, rains, and fast changes of ground cover are some of the constraint factors found. AVHRR is the only tool available for detection and monitoring of fires on a global basis—a much needed requirement in global, regional or local environmental studies. Most of the fires detected by AVHRR were validated in the TM images proving the potential use of this satellite sensor even in this vegetation type where it is less effective. For regions where no other fire detection capabilities exist AVHRR can provide a unique regular database of fire distribution and support operational fire fighting.

Acknowledgments

We acknowledge the support of Fundação de Ámparo a Pesquisa do Estado de São Paulo—FAPESP, which made the development of this work possible through grant no. 90/2950-2 for interdisciplinary projects.

References

AZEVEDO, L. G., and ADÁMOLI, J., 1988, Avaliação agroecológica dos recursos naturais da região dos cerrados. In *Proceedings of the 6th Simpósio sobre o Cerrado*, Brasília, DF, 1982 (Planaltina, DF: EMBRAPA-CPAC), pp. 729–761 (in Portuguese).

BELWARD, A. S., GRÉGOIRE, J. M., D'SOUZA, G., TRIGG, S., HAWKES, M., BRUSTET, J. M., SERCA, D., TIREFORD, J. L., CHRALOT, J. M., and VUATTOUX, R. 1993, *In situ*, real time fire detection using NOAA/AVHRR data. In *Proceedings of the 6th European AVHRR Data Users' Meeting, Belgirate, Italy* Dormstadt: EUMETSAT), pp. 333–339.

CHUVIECO, E., and CONGALTON, R. G., 1988, Mapping and inventory of forest fires from digital processing of TM data. *Photogrammetric Engineering and Remote Sensing*, **3**, 41–53.

COUTINHO, L. M. 1990, Fire in the ecology of Brazilian Cerrado. In *Fire in the tropical biota—ecosystem processes and global challenges*, edited by J.G. Goldammer (Berlin: Springer-Verlag), pp. 82–103.

CRUTZEN, P. J., and ANDREAE, M., 1990, Biomass burning in the tropics: impact on atmospheric chemistry and biogeochemical cycles. *Science*, **250**, 1669–1678.

DOZIER, J., 1981, A method for satellite identification of surface temperature fields of subpixel resolution. *Remote Sensing of Environment*, **11**, 221–229.

ENGESPAGO, 1988, *Sistema de tratamento de imagens—SITIM: manual do sistema* (São Jose dos Campos: INPE) (in Portuguese).

ESPINOZA, W., AZEVEDO, L. G., JARRETA JÚNIOR, M., 1982, O clima da região dos cerrados em relação à agricultura (Planaltina, DF: EMBRAPA-CPAC), 37 pp. Technical Circular no. 9 (in Portuguese).

IBGE/IBDF (INSTITUTO BRASILEIRO DE GEOGRAFIA E ESTATÍSTICA/INSTITUTO BRASILEIRO DE DESENVOLVIMENTO FLORESTAL), 1988, *Mapa de vegetação do Brasil* (Rio de Janeiro: IBGE), (in Portuguese).

IGBP (INTERNATIONAL GEOSPHERE AND BIOSPHERE PROGRAM) 1990, Report No. 13. Terrestrial biosphere exchange with global atmospheric chemistry, terrestrial biosphere perspective of the IGAC project. IGPB, Stockholm, Sweden.

KIDWELL, K. B., 1991, *NOAA polar orbiter data—users guide.* (Washington, DC: NOAA/NESDIS).

LANGAAS, S., 1992, Temporal and spatial distribution of savanna fires in Senegal and Gambia, West Africa, 1989–1990, derived from multi-temporal AVHRR night images. *International Journal of Wildland Fire*, **2**, 21–36.

PEREIRA JR., A. C., 1992, *Monitoramento de queimadas na região dos Cerrados utilizando dados AVHRR/NOAA corrigidos por dados TM/Landsat.* MSc Dissertation in Remote Sensing. (São José dos Campos: INPE), INPE-5490-TDI/507 (in Portuguese).

Downloaded By: [INSTITUTO NACIONAL DE PESQUISAS ESPACIAIS] At: 18:43 23 April 2010

PEREIRA, M. C., AMARAL, S., ZERBINI, N. J. and SETZER, A. W., 1990, Estimativa da área total queimada no Parque Nacional das Emas com o uso de imagens da banda 3 do AVHRR: comparação com estimativas do TM/Landsat. In *Proceedings of the 6th Simpósio Brasileiro de Sensoriamento Remoto, Manaus, AM, Brazil* (São José dos Campos: INPE), **Vol 2,** pp. 302–310 (in Portuguese).

PEREIRA JR., A. C., SETZER, A. W., and SANTOS, J. R., 1991, Fire estimates in savannas of central Brazil with thermal AVHRR/NOAA calibrated by TM/Landsat. In *Proceedings of 4th International Symposium on Remote Sensing of Environment R. Janeiro, RJ, Brazil* (Ann Arbor, MI: ERIM), pp. 825–836.

PEREIRA, M. C., and SETZER, A. W., 1993 a, Spectral characteristics of deforestation fires in NOAA/AVHRR images. *International Journal of Remote Sensing*, **14,** 583–597.

PEREIRA, M. C., and SETZER, A. W., 1993 b, Spectral characteristics of deforestation fires in Landsat-5/TM images. *International Journal of Remote Sensing*, **14,** 2061–2078.

PONZONI, F. J., LEE, D. C. L., and HERNADEZ FILHO, P., 1986, Avaliação da área queimada e de regeneração da vegetação afetada pelo fogo no Parque Nacional de Brasília através de dados TM/Landsat. In *Proceedings of 4th Simpósio Brasileiro de Sensoriamento Remoto, Gramado, RS, Brazil* (São José dos Campos: INPE), **Vol 1,** pp. 615–621, (in Portuguese).

SETZER, A. W., 1993, Operational satellite monitoring of fires in Brazil. *International Forest Fire News*, **9,** 8–11.

SETZER, A. W., and PEREIRA, M. C., 1991, Operational detection of fires in Brazil with NOAA/AVHRR. In *Proceedings of the 4th International Symposium on Remote Sensing of Environment, Rio de Janeiro, RJ, Brazil* (Ann Arbor, MI: ERIM), pp. 469–482.

SETZER, A. W., PEREIRA, M. C., and PEREIRA JR., A. C., 1992, O uso de satélites NOAA na detecção de queimadas no Brasil. *Climanálise*, **7,** 40–53 (in Portuguese).

SETZER, A. W., and MALINGREAU, J. P., 1993, Temporal variation in the detection limit of fires in AVHRR's channel 3. In *Proceedings of 6th European AVHRR Data Users' Meeting, Belgirate, Italy, 1993* (Dormstadt: EUMETSAT), pp. 575–579.

SETZER, A. W., and VERSTRAETE, M. M., 1994, Fire and glint in AVHRR's channel 3: a possible reason for the non-saturation mystery. *International Journal of Remote Sensing*, **15,** 711–718.

SETZER, A. W., PEREIRA, M. C., and PEREIRA JR., A. C., 1994, Satellite studies of biomass burning in Amazonia—some practical aspects. *Remote Sensing Reviews*, **10,** 91–103.

WARD, D. E., SUSOTT, R. A., KAUFFMAN, J. B., BABBIT, R. E., CUMMINGS, D. L., DIAS, B., HOLBEN, B. N., KAUFMAN, Y. J., RASMUSSEN, R. A., and SETZER, A. W., 1992, Smoke and fire characteristics for Cerrado and deforestation burns in Brazil: BASE-B experiment. *Journal of Geophysical Research*, **97,** 14601–14619.

Downloaded By: [INSTITUTO NACIONAL DE PESQUISAS ESPACIAIS] At: 18:43 23 April 2010